

# Chlorin-Oligonucleotide Conjugates: Synthesis, Properties, and Red Light-Induced Photochemical Sequence-Specific DNA Cleavage in Duplexes and Triplexes<sup>†,‡</sup>

Alexandre S. Boutorine,<sup>§</sup> Daniel Brault,\* Masashi Takasugi, Olavio Delgado, and Claude Hélène

Contribution from the Laboratoire de Biophysique, INSERM U201, CNRS URA 481, Muséum National d'Histoire Naturelle, 43 rue Cuvier, 75231 Paris Cedex 05, France

Received January 8, 1996<sup>⊗</sup>

**Abstract:** Conjugates of oligonucleotides with chlorin-type photosensitizers were prepared. Two chlorin moieties, CPP and CHEVP, characterized by a modified pyrrole unit bearing an aldehyde chain, were photochemically prepared from protoporphyrin and heptaethylvinylporphyrin, respectively. These chlorin moieties were coupled through the carboxylic acid side-chain (CPP) or aldehyde side-chain (CHEVP) to the 3'-activated phosphate of oligodeoxynucleotides. Diamine or dihydrazide were used as linkers. The resulting conjugates were purified by HPLC and characterized by electrophoresis, UV-visible spectroscopy, and mass spectrometry. The photosensitizing properties of the conjugate of CHEVP with the 14-mer oligodeoxynucleotide TTCTTCTCCTTTCT were investigated using three different targets. A single-stranded 25-mer containing the complementary sequence of the 14-mer formed a double helix with the chlorin-14-mer conjugate. A 24 base-pair duplex and a 41-mer hairpin with 18 base pairs and a five nucleotide loop formed triple helices with the conjugate. In all cases, upon irradiation with visible light (428 or 668 nm), piperidine-labile sites at guanine positions were produced. The reaction required oxygen and was inhibited to some extent by sodium azide. The cleavage sites were correlated with the chlorin position in both the duplex and triplex structures. In the 41-mer hairpin, the most reactive guanines were those located in the loop region. The quantum yield for cleavage of the hairpin structure was determined to be about  $10^{-3}$ , independent of the excitation wavelength. This modest value is largely compensated by the high absorption of the chlorin in the red, making the conjugate highly efficient even under low light fluence. No effect was found with a noncomplementary chlorin-oligonucleotide conjugate. These results show that site-directed damages to nucleic acid structures can be achieved using oligonucleotide-chlorin conjugates and red light irradiation.

## Introduction

The artificial control of gene expression by synthetic oligonucleotides has been the subject of considerable interest in the recent years. Oligonucleotides can bind to a complementary sequence on a messenger RNA and inhibit translation of the mRNA information into a polypeptide chain (the antisense approach). Alternatively, oligonucleotides can form triple helical complexes with double stranded DNA and inhibit gene transcription (the antigene strategy). These approaches have been reviewed recently.<sup>1–3</sup> In addition, it was recently shown that the range of possible targets for oligonucleotides could be considerably extended. Indeed, the SELEX (or aptamer) technology makes it possible to identify oligonucleotide sequences with high affinity for an unexpected variety of proteins.<sup>4</sup>

The activity of oligonucleotides first relies on their binding to their target (whatever it may be), a process which is reversible.

Composite molecules associating oligonucleotides with reactive substituents have been designed in order to produce irreversible damages in the target.<sup>3,5</sup> Chemically active substituents have been found to be efficient in vitro.<sup>5</sup> Their use for in vivo applications is limited, however, because they may react with various biological components, which could result both in an undesirable toxicity, and in a drastic reduction of the amount of the derivative reaching its target. Also, the mechanism of action of chemically active substituents may require a co-reagent, a condition hardly compatible with in vivo applications.

Advantage might be found in substituents which are not toxic in the dark but can be activated by light. Their action could be controlled within space and time by proper irradiation protocols. This approach is reminiscent of photochemotherapy which is currently under evaluation in the treatment of tumors<sup>6</sup> as well as in emerging applications such as virus photoinactivation in blood products.<sup>7</sup> Oligonucleotides linked to various photoactive molecules have been shown to induce sequence specific damages to target nucleic acids in vitro.<sup>8–13</sup> An important

\* FAX: 33 1 40 79 37 05.

<sup>§</sup> Present address: GENTA Pharmaceuticals Europe, 163 Avenue de Luminy, case 902, 13288 Marseille Cedex 09, France.

<sup>†</sup> Keywords: Oligonucleotide, chlorin, conjugate, duplex, triplex, light-induced cleavage, quantum yield.

<sup>‡</sup> Abbreviations: CHEVP: chlorin derived from heptaethylvinylporphyrin, CPP: chlorin derived from protoporphyrin, CTAB: hexadecyltrimethylammonium bromide.

<sup>⊗</sup> Abstract published in *Advance ACS Abstracts*, September 15, 1996.

(1) Hélène, C.; Toulmé, J. J. *Biochim. Biophys. Acta* **1990**, *1049*, 99–125.

(2) Uhlmann, E.; Peyman, A. *Chem. Rev.* **1990**, *90*, 543–584.

(3) Thuong, N. T.; Hélène, C. *Angew. Chem., Int. Ed. Engl.* **1993**, *32*, 666–690.

(4) Gold, L.; Poliski, B.; Uhlenbeck, O.; Yarus, M. *Annu. Rev. Biochem.* **1995**, *64*, 763–797.

(5) Knorre, D. G.; Vlassov, V. V.; Zarytova, V. F.; Lebedev, A. V.; Fedorova, O. S. *Design and targeted reactions of oligonucleotide derivatives*; CRC Press: Boca Raton, FL, 1994.

(6) *Photodynamic Therapy of Neoplastic Disease*; Kessel, D., Ed.; CRC Press: Boston, 1990.

(7) Matthews, J. L.; Newman, J. T.; Sogandares-Bernal, F.; Judy, M. M.; Skiles, H.; Leveson, J. E.; Marengo-Rowe, A. J.; Chanh, T. C. *Transfusion* **1988**, *28*, 81–83.

(8) Praseuth, D.; Le Doan, T.; Chassignol, M.; Decoux, J.-L.; Habhoub, N.; Lhomme, J.; Thuong, N. T.; Hélène, C. *Biochemistry* **1988**, *27*, 3031–3038.

(9) Le Doan, T.; Praseuth, D.; Perrouault, L.; Chassignol, M.; Thuong, N. T.; Hélène, C. *Bioconjugate Chem.* **1990**, *1*, 108–113.

concern for the development of this class of compounds is the penetration of light within tissues or blood which act as screens below 600 nm.<sup>14</sup> In the present paper, we describe methods for coupling oligonucleotides to red-absorbing photosensitizers belonging to the family of chlorins.<sup>15</sup> Upon irradiation with red-light in the presence of oxygen, these conjugates are shown to efficiently induce sequence-specific damages to single-stranded or double-stranded nucleic acids.

## Materials and Methods

**Reagents.** Organic solvents and inorganic salts were purchased from Aldrich, Merck or Sigma. Hexadecyltrimethylammonium bromide (CTAB) was from Sigma. Adipic acid dihydrazide, 2,2'-dipyridyldisulfide, triphenylphosphine, and 4-dimethylaminopyridine were from Aldrich. Hexamethylenediamine was from Merck. Deuterium oxide (99.8%) was from Euriso-top, France, and high purity argon ( $O_2 < 0.5$  ppm) from Air Liquide, France. Oligodeoxyribonucleotides were synthesized by Eurogentec. Phosphorylation of oligonucleotides was carried out with T4 polynucleotide kinase (Ozyme) according to a protocol modified as described previously.<sup>16</sup> Electrospray mass spectra were recorded on a VG platform (Fisons) at the Service central d'analyse CNRS, Solaise, France. The sample was dissolved in water/2-propanol.

**Synthesis of the Chlorin-Type Photosensitizers.** Two chlorin-type photosensitizers were prepared photochemically from vinyl porphyrins as described elsewhere.<sup>15</sup> Briefly, in oxygenated solutions, the porphyrin induces its own transformation upon light irradiation by sensitizing the formation of singlet oxygen. This species attacks the vinyl chain of the porphyrin leading to an endocyclic intermediate which rearranges to yield a modified pyrrole unit bearing formylmethylidene and hydroxyl chains.<sup>17</sup>

The two vinyl porphyrins used as starting materials were protoporphyrin (PP) and heptaethylvinylporphyrin (HEVP). The corresponding chlorin compounds will be referred to as CPP and CHEVP, respectively. Protoporphyrin was purchased from Aldrich. As PP possesses two vinyl groups, the photochemical reaction yields two isomers depending on the vinyl chain being modified. Their separation was not attempted. The structure of the two isomers of CPP (also known as photoporphyrin) is shown in Figure 1. HEVP was prepared from octaethylporphyrin (Aldrich) according to Bonnett et al.<sup>18</sup> As this symmetrical porphyrin possesses only one vinyl chain, a single chlorin product was formed. Its structure is shown in Figure 2. The chlorin compounds were separated from the unreacted porphyrins and side products by low pressure chromatography on silica. Their purity was typically better than 95% as shown

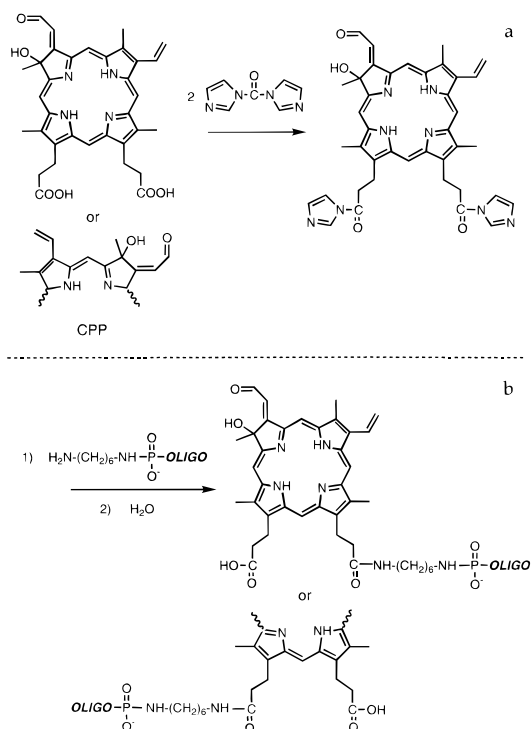


**Figure 1.** Scheme for coupling CPP with amino-derivatized oligonucleotides via an amide bond.

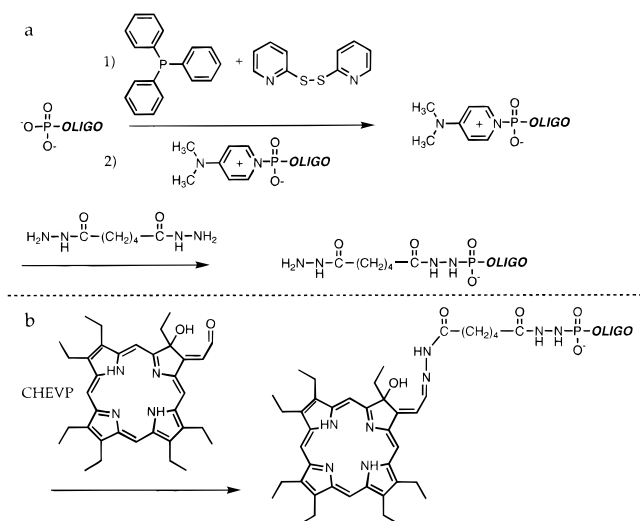


**Figure 2.** Scheme for derivatization of phosphorylated oligonucleotides with a dihydrazide linker and subsequent coupling with CHEVP.

by HPLC. Full details on the preparation and the characterization of these compounds will be given elsewhere.

**Synthesis of CPP-Oligonucleotide Conjugates Involving Carboxylic Chains. Derivatization of Oligonucleotides with an Amino Group.** The activation of the terminal phosphate of the oligonucleotide and the subsequent coupling with a diamine linker was carried out as described earlier,<sup>16</sup> except that *N*-methylimidazole was replaced by 4-dimethylaminopyridine. In short, the oligonucleotide, as its CTAB salt, was first allowed to react with 2,2'-dipyridyldisulfide, triphenylphosphine, and 4-dimethylaminopyridine in dry dimethylsulfoxide for 15 min. A 100-fold molar excess of hexamethylene diamine was then added to the activated phosphate, and the reaction pursued for 20 min at room temperature. The final product was precipitated by ethanol and washed thoroughly. It was analyzed by electrophoresis on a 20% denaturing polyacrylamide gel. Bands were visualized by UV-shadowing. The reaction yield was more

(10) Perrouault, L.; Asseline, U.; Rivalle, C.; Thuong, N. T.; Bisagni, E.; Giovannangeli, C.; Le Doan, T.; Hélène, C. *Nature* **1990**, *344*, 358–360.

(11) Boutorine, A. S.; Tokuyama, H.; Takasugi, M.; Isobe, H.; Nakamura, E.; Hélène, C. *Angew. Chem., Int. Ed. Engl.* **1994**, *33*, 2462–2465.

(12) Mastruzzo, L.; Woisard, A.; Ma, D. D. F.; Rizzarelli, E.; Favre, A.; Le Doan, T. *Photochem. Photobiol.* **1994**, *60*, 316–322.

(13) An, Y.-Z.; Chen, C.-H. B.; Anderson, J. L.; Sigman, D. S.; Foote, C. S.; Rubin, Y. *Tetrahedron* **1996**, *52*, 5179–5189.

(14) Wilson, B. C.; Jeeves, W. P.; Lowe, D. M. *Photochem. Photobiol.* **1985**, *42*, 153–162.

(15) Brault, D.; Aveline, B.; Delgado, O.; Vever-Bizet, C. *SPIE Proceedings Series: Photodynamic Therapy of Cancer* **1994**, *2325*, 40–46.

(16) Boutorine, A. S.; Le Doan, T.; Battioni, J. P.; Mansuy, D.; Dupré, D.; Hélène, C. *Bioconjugate Chem.* **1990**, *1*, 350–356.

(17) Aveline, B.; Delgado, O.; Brault, D. *J. Chem. Soc., Faraday Trans.* **1992**, *88*, 1971–1976.

(18) Bonnett, R.; Campion-Smith, I. H.; Kozyrev, A. N.; Mironov, A. *F. J. Chem. Research (M)* **1990**, 1015–1043.

than 90%, and no additional purification was performed. All the oligonucleotides used in the present study were derivatized at the 3' position of the terminal nucleotide.

**Coupling of CPP.** The carboxylic chains of CPP were activated as described by Gottikh et al.,<sup>19</sup> but carbonyl diimidazole was used as activating agent instead of 1-ethyl-3-(3'-dimethylaminopropyl)carbodiimide. CPP (2–3 mg) dissolved in 45  $\mu$ L of dry dimethylformamide was allowed to react with 5-fold molar excess of carbonyl diimidazole. After 10 min, the carbonyl diimidazole in excess was decomposed by addition of 5  $\mu$ L of 1 M triethylammonium borate buffer, pH 10.8. Then, 100–300  $\mu$ g of the amino-derivatized oligonucleotide in 15  $\mu$ L of the same buffer was added, and the solution was incubated for 8 h at room temperature. The solution was then diluted with water, and the unreacted chlorin was extracted by butanol until the extracts were colorless. The oligonucleotide conjugate was precipitated by ethanol and purified by HPLC on Lichrosorb C18 using a linear gradient of acetonitrile 5–80%. The conjugate was eluted with 40% acetonitrile. The conversion of the oligonucleotide to its conjugate was about 30–40% as deduced from the HPLC profile at 260 nm. A scheme of the conjugate synthesis is shown in Figure 1.

**Synthesis of Chlorin-Oligonucleotide Conjugates Involving Aldehyde Chain. The Dihydrazone Method.** Adipic acid dihydrazone (6 mg) dissolved in 100  $\mu$ L of dimethylsulfoxide at 50 °C was added to a dimethylsulfoxide solution of oligonucleotide activated at the terminal phosphate as described above. The mixture was incubated for 20 min, and the hydrazone derivative of oligonucleotide was precipitated using acetone containing 3% LiClO<sub>4</sub>. The pellet was washed with acetone redissolved in water and precipitated again with ethanol. The dry pellet was dissolved in 25  $\mu$ L of water, and the oligonucleotide derivative was precipitated using a 8% CTAB aqueous solution. The pellet was thoroughly dried and dissolved in water-free dimethylsulfoxide, and 2 mg of CHEVP in 200  $\mu$ L of dimethylsulfoxide was added to the solution. The mixture was incubated overnight at room temperature in the presence of dry molecular sieves. The chlorin-oligonucleotide conjugate was precipitated from the mixture using 3% LiClO<sub>4</sub> in acetone, washed by acetone, redissolved in water, and precipitated again with ethanol. The product was analyzed by HPLC on Lichrosorb C18 column using a 5–80% linear gradient of acetonitrile. A typical elution profile is shown in Figure 3a. The conjugate (retention time 18.7 min) was identified from its absorption at 400 or 670 nm and was well separated from the starting oligonucleotide (retention time 8.5 min). It was eluted as a single peak which was collected. Its purity was further checked by electrophoresis on a 20% denaturing polyacrylamide gel. The conjugate was found to move as a single spot which showed the characteristic red fluorescence of the chlorin moiety under excitation at 365 nm. No other band or smear around the conjugate spot was visualized by UV shadowing using 254 nm light. Negative electrospray ionization mass spectrometry of the conjugate revealed a pattern of peaks consistent with multiply charged species associated to various numbers of sodium and/or potassium ions. The mass thus deduced (4904.8) was in good agreement with the calculated mass of the conjugate (4904.6). A scheme of the conjugate synthesis is shown in Figure 2. The absorption spectrum of the conjugate is shown in Figure 3b.

**The Diamine Method. Derivatization of CHEVP with an Amino Group.** The reaction between the aldehyde group of CHEVP and hexamethylene diamine was carried out in anhy-

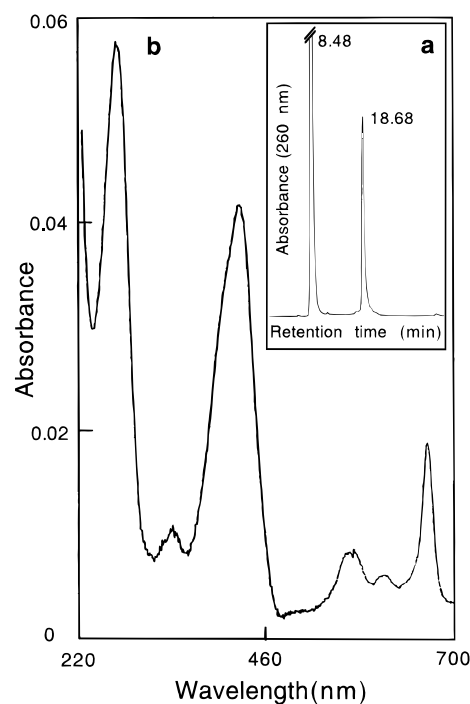


**Figure 3.** (a) HPLC profile of the product of the reaction between the TTCTTCCTTCT oligonucleotide and CHEVP according to the scheme shown in Figure 2. (b) Absorption spectrum of the purified TTCTTCCTTCT-CHEVP conjugate in 0.01 M tris-HCl, pH 7.6.

drous tetrahydrofuran. CHEVP (10 mg) was dissolved in a minimal amount of tetrahydrofuran (about 1 mL), and the solution was added with dry molecular sieves (Merck). Then, 20  $\mu$ L of melted hexamethylene diamine, followed by 1 mg of sodium borohydride, was added under agitation. The reaction mixture was incubated overnight at room temperature under slight agitation. After addition of 5 mL of chloroform, the diamine in excess was extracted by water. After complete elimination of the diamine, as controlled by the ninhydrin reaction on the water phase, the organic phase was dried under vacuum. The reaction product was analyzed by thin layer chromatography on silica gel 60 using a mixture of chloroform (80%) and ethanol (20%) as eluant. Unreacted CHEVP migrated with the front of the solvent, whereas the amino-derivatized compound remained at the origin.

**Conjugation of the CHEVP Amino Derivative with the Oligonucleotide.** The oligonucleotide terminal phosphate was activated as described above. The amino derivative of CHEVP was attached to the activated phosphate in the presence of triethylamine as described previously.<sup>16</sup> The resulting conjugate was precipitated by 3% lithium perchlorate in acetone, washed by acetone, dissolved in water, and purified on a Lichrosorb C18 HPLC column using a 5–80% linear gradient of acetonitrile. The CHEVP-oligonucleotide conjugate was eluted with 60% acetonitrile. The yield of the reaction was 70–80%. The conjugate was characterized by absorption spectroscopy, and its purity was characterized by denaturing electrophoresis on a 20% polyacrylamide gel as described above. The scheme of the conjugate synthesis is shown in Figure 4.

**Complex Formation between the Conjugate and Its Target.** The targeted sequences and structures formed are shown in Figure 5. As compared to a previous study using a fullerene-oligonucleotide conjugate,<sup>11</sup> the single strand and duplex targets (1 and 2 in Figure 5) did not contain G tracks in order to avoid undesired quadruplex formation.<sup>20</sup> Moreover, this sequence

(19) Gottikh, M. B.; Ivanovskaya, M. G.; Skripkin, E. A.; Shabarova, Z. A. *Bioorg. Khimika* **1990**, *16*, 514–523.

(20) Sen, D.; Gilbert, W. *Nature* **1988**, *334*, 364–366.

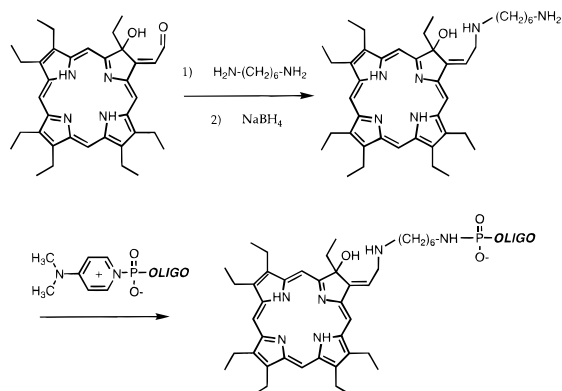


**Figure 4.** Scheme of synthesis of oligonucleotide-CHEVP conjugate by the diamine method.

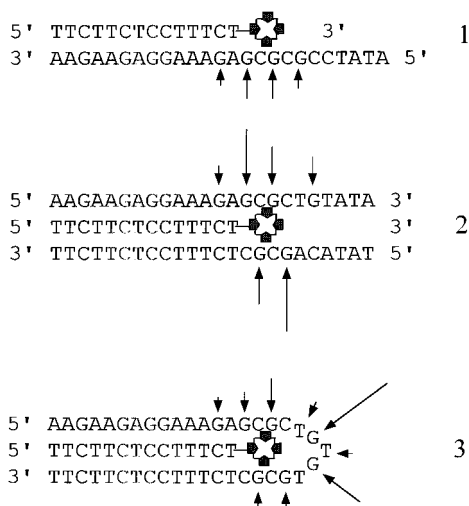


**Figure 5.** Complexes of the oligonucleotide-chlorin conjugate with different targets: 1 - duplex with complementary oligonucleotide, 2 - triple helix, 3 - triple helix with hairpin structure. The arrows indicate sites which are specifically cleaved upon light irradiation and subsequent piperidine treatment. These sites are identified by the initial dependence of the cleavage efficiency on the irradiation time. The arrow lengths correspond to the intensity of photoinduced cleavage.

changes made it possible to check the cleavage efficiency on both chains of the duplex target with minimal bias due to sequence differences. A 41-mer hairpin structure with a five base loop was also investigated (see structure 3 in Figure 5).

The target oligonucleotides were 5'-labeled with  $\gamma$ - $^{32}\text{P}$ -phosphate. Complexes between the conjugate and its targets were formed in 10 mM sodium cacodylate buffer, pH 6.0, containing 50 mM NaCl. In the case of triple helix formation, 0.25 mM spermine was added, and the conjugate was incubated with its target overnight at 4 °C. The concentrations of the target and the conjugate were in the range of 50–300 nM and 3–5  $\mu\text{M}$ , respectively. In some cases, the solution containing the preformed complex was concentrated to dryness and then redissolved in  $\text{D}_2\text{O}$ . In other experiments, sodium azide was added to the solution.

**Irradiation of Complexes.** Irradiations were carried out using a 1000 W xenon arc mounted in a lamp housing equipped with a rear reflector and a 3 in. diameter fused silica condenser of  $f/0.7$  aperture (Oriel). After elimination of infrared light by a water filter, the beam was focused at the entrance of a monochromator (Bentham M300). The entrance and exit slits were set at 4 mm to produce a narrow irradiation band of 11 nm width. Two wavelengths, 668 and 428 nm were selected to match the main absorption bands of the oligonucleotide-conjugate in the red and the Soret regions, respectively. A long

wavelength-pass glass filter (Schott GG375) was put at the monochromator exit to eliminate UV light arising from second order diffraction. A 100 mm focal lens was used to form the image of the monochromator exit slit on a thermostated cell holder. The image was a square of about  $10 \times 10$  mm. For quantum yield determination, the irradiated solution was contained in a quartz micro cell (Hellma) with an optical path length of 1.5 mm. The cell entrance window ( $1.5 \times 5$  mm) was placed in the center of the illuminated area where the light intensity was uniform. The light intensity was measured in the working area using a power meter (surface-absorbing disc calorimeter from Scientech). The volume of the sample was 10  $\mu\text{L}$ . Thus, all the sample was contained in the irradiated volume of the cell. The light intensity received by the solution (after correction for the transmission of the front face of the cell) was 12.6 and 16.4  $\text{mW}/\text{cm}^2$ , i.e.,  $2.71 \times 10^{16}$  and  $5.51 \times 10^{16}$  photons  $\text{s}^{-1} \text{cm}^{-2}$  at 428 and 668 nm, respectively. A neutral filter (Schott NG4) reducing the intensity by a factor of 9.61 was used for experiments aimed at investigating low photocleavage ratios in detail. A new 10  $\mu\text{L}$  sample was used for each irradiation time. An alternative procedure was used in preliminary experiments. A single sample of 150  $\mu\text{L}$  contained in a standard 1 mm path length cell was irradiated, and 10  $\mu\text{L}$  aliquots were taken out after various times. All the solution was irradiated by adjusting the size of the illuminated area. However, the uniformity of light distribution was less than in the former procedure. Nevertheless, both protocols gave qualitatively the same results. The optical cells were treated with silicone to avoid adsorption of the conjugate on quartz. Some other experiments were carried out on samples contained in capillary quartz tubes using a bench equipped with a 150 W Xenon lamp. In this case, the infrared light was eliminated using a dichroic filter and the UV light below 310 nm by a long wavelength pass filter. All the experiments were performed at 10 °C.

For experiments involving anaerobic conditions, the solution contained in the optical cuvette was bubbled, for more than 1 h before irradiation, with argon using a capillary tube. The gas was saturated with the solvent which was kept at the same temperature as the solution to avoid evaporation.

In order to reveal some of the hidden base damages in the target, half of each sample was treated with 1 M piperidine for 30 min at 90 °C. The samples (treated or not with piperidine) were analyzed by electrophoresis in denaturing gel (20% acrylamide, 7 M urea). Autoradiographs and quantitative data were obtained from a Phosphor Imager (Molecular Dynamics).

The oligonucleotide TTCTTCTCCTTTCTp without a chlorin group and the noncomplementary oligonucleotide CGGCAGC-CACACp with a chlorin group attached at the 3'-terminus were used as controls.

**Determination of the Photochemical Quantum Yield of Cleavage.** The photochemical quantum yield of cleavage,  $\Phi$ , is defined as the ratio of the number of cleaved sites ( $n_{\text{cs}}$ ) versus the number of absorbed photons ( $I_{\text{a}}$ ). In our experiments, the concentration ( $C$ ) of the absorbing species, i.e., the oligonucleotide-chlorin conjugate, was 5  $\mu\text{M}$  and the optical path length of the cuvette ( $l$ ), 1.5 mm. The absorbance of the solutions at 668 or 428 nm did not exceed 0.05. Therefore, a simplified form of Beer's law holds<sup>21</sup>

$$I_{\text{a}} = 2.3I_0\epsilon Cl \quad (1)$$

where  $I_0$  is the total number of incident photons and  $\epsilon$  the molar extinction coefficient of the conjugate at the irradiation wave-

(21) Parker, C. A. *Photoluminescence of Solutions*; Elsevier: Amsterdam, 1968.

length. Furthermore, as all the sample was contained within the volume irradiated in the optical cuvette, the concentration  $C$  can be expressed as

$$C = n_{\text{abs}}/(NSI) \quad (2)$$

where  $n_{\text{abs}}$  is the number of absorbing molecules,  $N$  is the Avogadro number, and  $S$  is the surface occupied by the solution at the front face of the cell. Then,

$$I_a = 2.3I_{0s}\epsilon n_{\text{abs}}/N \quad (3)$$

where  $I_{0s}$  is the number of incident photons per surface unit. From the above equations, the photochemical yield can be expressed as

$$\Phi = N(n_{\text{cs}}/n_{\text{abs}})/(2300I_{0s}\epsilon) \quad (4)$$

where  $I_{0s}$  is expressed as a number of photons per  $\text{cm}^2$  (a conversion factor of 1000 is introduced to take into account the fact that  $\epsilon$  units are  $\text{M}^{-1} \text{cm}^{-1}$ , i.e.,  $\text{mol}^{-1} \text{cm}^{-1} \text{dm}^3$ ).

As shown in the result section, cleavage occurs only in the 1/1 complex between the oligonucleotide and its target. Thus,  $n_{\text{cs}}/n_{\text{abs}}$  can be expressed as the ratio of the radioactivity counted in the bands corresponding to cleaved oligonucleotides versus the total radioactivity, i.e.,

$$\Phi = NP_r/(2.3 \times 10^5 I_{0s}\epsilon) \quad (5)$$

where the photocleavage ratio,  $P_r$ , is expressed in percentage.

## Results

**Synthesis of Chlorin-Oligonucleotide Conjugates.** Several methods were developed to attach oligonucleotides to the chlorin molecules by making use of different functional groups carried by the chlorin macrocycle. The preparation of oligonucleotides linked to porphyrins has been well exemplified in various protocols.<sup>9,12,16,22,23</sup> Thus, the simplest approach was to use groups already present in the vinyllic porphyrin used to prepare the chlorin molecule, such as the propionic acid chains in CPP (see Figure 1). As CPP bears two carboxylic groups, it was necessary to work with an excess of the activated chlorin in order to get the 1/1 conjugate. The second carboxylic group of CPP was recovered by hydrolysis after the coupling step. This group as well as the polar chains of the modified pyrrole unit provide some hydrophilic character to the chlorin moiety of the conjugate as compared to the conjugate with CHEVP which is described below.

Two isomers of the conjugate with CPP were obtained, depending on the chain involved in the linkage. In addition, CPP itself was composed of two isomers according to the position of the modified pyrrole (see Figure 1). The HPLC peak of the conjugate was quite broad, and it was not possible to separate the various isomers.

Alternative approaches were therefore sought. It is worth noting that the route used to prepare the chlorin molecules under study<sup>15,17</sup> leads to a modified pyrrole bearing an aldehyde chain amenable to coupling procedure via Schiff base formation with primary amines.

In order to avoid problems related to the presence of various isomers, we used the chlorin CHEVP (Figure 2) derived from heptaethylvinylporphyrin. The direct reaction of CHEVP with oligonucleotides derivatized with an amino function (as in the

former protocol) did not give satisfactory results, even if sodium borohydride was used to reduce the Schiff base. Instead, we investigated a coupling procedure involving the more reactive hydrazide function. Oligonucleotides were first derivatized by linking adipic acid dihydrazide to the 3' terminal phosphate (Figure 2). The yield of the oligonucleotide hydrazide derivative was 70–80%. Then, this derivative was converted to its CTAB salt which was soluble in organic solvents. The coupling with the chlorin was carried out in dry dimethylsulfoxide. A green-colored water-soluble conjugate was obtained and purified by HPLC. The yield of the conjugate based on the dihydrazide oligonucleotide derivative was around 25%.

The conjugate was stable, no alteration being observed during storage for one year. No stabilization through reduction of the imine bond by sodium borohydride was required. The conjugate was further characterized by electrophoresis in 20% denaturing polyacrylamide gel. It moved as a single band, a little slower than the initial oligonucleotide. Under UV-irradiation at 365 nm, this band revealed the characteristic red fluorescence of the chlorin moiety.

The absorption spectrum of the conjugate of CHEVP with the oligonucleotide TTCTTCTCCTTTCT is reported in Figure 3b. As expected, it shows both the characteristics of the chlorin moiety with a red band at 668 nm and a Soret band around 428 nm, and those of the oligonucleotide part with a peak around 265 nm. The ratios between the intensity of the 265 nm band and that of the Soret band on one hand, or the red band on the other hand (1.4 and 3.0, respectively) confirm the 1:1 chlorin-oligonucleotide composition of the conjugate.

The CHEVP-conjugate appears to be more hydrophobic than the CPP-conjugate as judged by the percentage of acetonitrile required to elute them in HPLC (60 and 40%, respectively). In fact, the hydrophobicity of the CHEVP-conjugate can be compared to the conjugates of oligonucleotides with cholesterol.<sup>16</sup>

In order to improve the yield of the conjugate, a second coupling procedure involved the derivatization of CHEVP as well as the activation of the oligonucleotide. The reaction scheme is depicted in Figure 4. First, we synthesized an amino derivative of CHEVP by incubating this chlorin, in absolutely dry conditions, with an excess of hexamethylene diamine in the presence of sodium borohydride. Thin layer chromatography analysis (not shown) demonstrated almost complete conversion of CHEVP into its diamine derivative (the fluorescence spot of the initial CHEVP was hardly visible under UV excitation). This derivative was purified from diamine excess and then dried as fully described in the Materials and Methods section. Then, it was coupled to the oligonucleotide which was previously activated at its 3' terminal phosphate by dimethylaminopyridine. As estimated from electrophoresis and HPLC, the conjugate is formed with a yield of 80% relative to the initial oligonucleotide. This oligonucleotide-chlorin conjugate showed HPLC, electrophoretic, and spectroscopic characteristics very similar to those displayed by the oligonucleotide-chlorin conjugate obtained by the hydrazide method (results not shown).

**Site-Directed Photochemical Cleavage of DNA.** The experiments were carried out with the 14-mer oligonucleotide TTCTTCTCCTTTCT coupled to CHEVP using the hydrazide method. We investigated the photochemical effect of this conjugate on target oligodeoxynucleotides in three different structures. As illustrated in Figure 5, the target was either a single-stranded 25 mer containing the complementary sequence of the conjugate, a duplex with 24 base pairs and a 41-mer hairpin structure with 18 base pairs and a five nucleotide single-stranded loop. In the two last cases, triplex structures are formed

(22) Le Doan, T.; Perrouault, L.; Hélène, C.; Chassignol, M.; Thuong, N. T. *Biochemistry* **1986**, *25*, 6736–6739.

(23) Casas, C.; Lacey, C. J.; Meunier, B. *Bioconjugate Chem.* **1993**, *4*, 366–371.

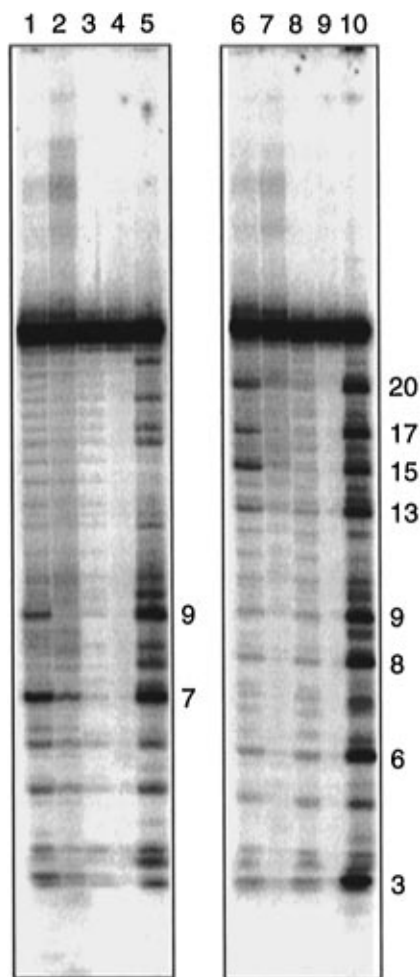


**Figure 6.** Electrophoretic analysis of the photocleavage of double-stranded oligonucleotide (Figure 5, structure 2). The photoactive agent was the TTCTTCTCCTTTCT-CHEVP conjugate (prepared according to the scheme shown in Figure 2) which forms a triple helix with its target. The two strands were  $^{32}\text{P}$ -labeled and analyzed in independent experiments. The samples were irradiated for 10 min using the visible spectrum of a 150 W xenon lamp. 1–5, pyrimidine-containing strand; 6–10, purine-containing strand; 5, 10, G-ladder (treatment with dimethylsulfate followed by 30 min heating with 1 M piperidine at 100 °C). The duplex target was irradiated in presence (1, 2, 6, 7) or absence (3, 4, 8, 9) of the chlorin-oligonucleotide conjugate. The irradiated samples were treated (1, 3, 6, 8) or not (2, 4, 7, 9) with piperidine. The positions of guanine residues are indicated in the 5'–3' direction.

between the oligonucleotide-chlorin conjugate and its target.<sup>24</sup> Site-directed damages were observed in the three different targets as summarized in Figure 5. Results will be presented in more detail for the triple helix structures.

Damages on the targets  $^{32}\text{P}$ -labeled at the 5'-end were analyzed by electrophoresis on denaturing gels. In Figure 6 are shown results obtained with the 24-mer double stranded target. Each strand was labeled in independent experiments. The duplex was irradiated either in the absence (control) or in the presence of the oligonucleotide-chlorin conjugate. In each case, the sample was treated or not with piperidine before the electrophoresis. For both strands, some site directed cleavages were observed at guanine positions on untreated samples. Piperidine-treatment significantly increased the amount of cleavage which was observed at well defined sites as shown in

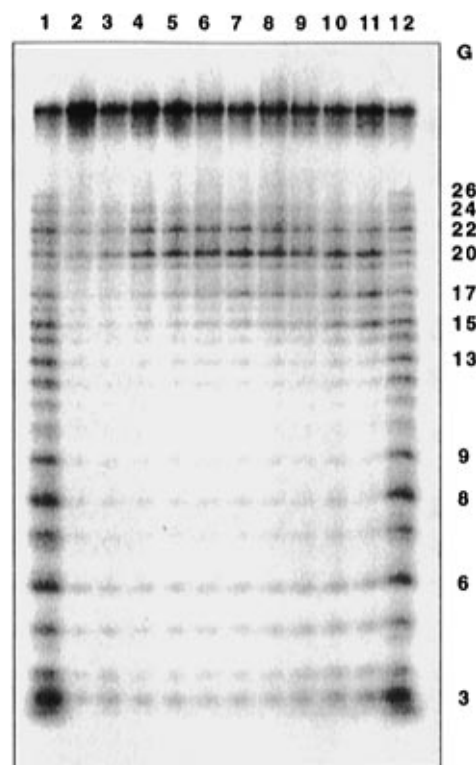


**Figure 7.** Electrophoretic analysis of the photocleavage of  $^{32}\text{P}$ -labeled double-stranded oligonucleotide with hairpin structure (Figure 6, structure 3). The photoactive agent was the TTCTTCTCCTTTCT-CHEVP conjugate (prepared according to the scheme shown in Figure 2) which forms a triple helix with its target. 1, 12: G-ladder (treatment of the labeled double-stranded 41-mer with dimethylsulfate followed by 30 min heating with 1 M piperidine at 100 °C.); 2–11, complex irradiated for 0, 1, 2.5, 5, 7.5, 10, 15, 25, 40, 60 min and subsequently treated with piperidine. The concentrations of the conjugate and the target were 5  $\mu\text{M}$  and 270 nM, respectively. The pH 6 buffered solution contained 10 mM sodium cacodylate, 50 mM NaCl and 0.25 mM spermine. Irradiation was performed with 668 nm light (16.4 mW/cm<sup>2</sup>). Electrophoresis was carried out in 20% denaturing polyacrylamide gel. The positions of guanine residues are indicated in the 5'–3' direction.

Figure 6. Photoadducts were also formed as revealed by slow migrating bands in the untreated samples (see Figure 6). They were assigned to monoadducts using size markers. These bands were extracted from preparative gels and subjected to piperidine treatment. The cleavage pattern thus obtained was very similar to that observed with the initial samples. This suggests that a part of the cleavage observed at well defined guanine sites arises from piperidine-labile photoadducts.

The kinetics of cleavage was investigated in more detail on the hairpin target. Again, piperidine-treatment significantly increased the cleavage. A typical autoradiogram obtained after piperidine treatment is shown in Figure 7. Three important features can be qualitatively observed: (i) the cleavage efficiency depends on the irradiation time, (ii) major damages are site-directed and arise close to the expected location of the chlorin molecule, and (iii) cleavage occurs predominantly at guanines although thymines 19 and 21 in the single stranded-loop present some reactivity. The same cleavage pattern was observed whether the irradiation was performed using 668 or 428 nm light or the full light spectrum above 310 nm. In Figure 8 is depicted, for two wavelengths, the time dependence of site-directed cleavage (positions 13 to 26) of the 41-mer hairpin before and after piperidine treatment. Results from three independent experiments normalized as a function of photons received by the solutions are depicted in Figure 9. It is worth

(24) Mergny, J. L.; Duval-Valentin, G.; Nguen, C. H.; Perrouault, L.; Faucon, B.; Rougée, M.; Montenay-Garestier, T.; Bisagni, E.; Hélène, C. *Science* **1992**, 256, 1681–1684.

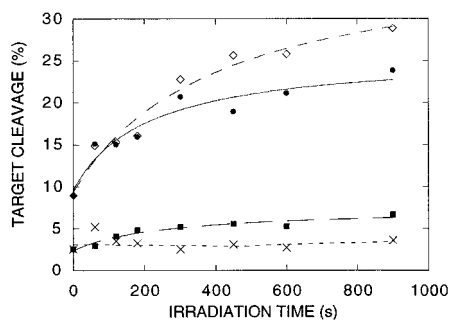


**Figure 8.** Kinetics of site-directed cleavage (positions 13–26) of the 41-mer hairpin by the TTCTTCTCCTTCT-CHEVP conjugate before (lower curves) and after (upper curves) piperidine treatment. Irradiation was performed at 668 nm (■, ●) or at 428 nm (×, ◇). The light intensity was  $5.73 \times 10^{15}$  at 668 nm and  $2.82 \times 10^{15}$  photons  $s^{-1} cm^{-2}$  at 428 nm. The results after piperidine treatment have been fitted with curves corresponding to  $y = ax/(bx + 1) + c$  (see text).

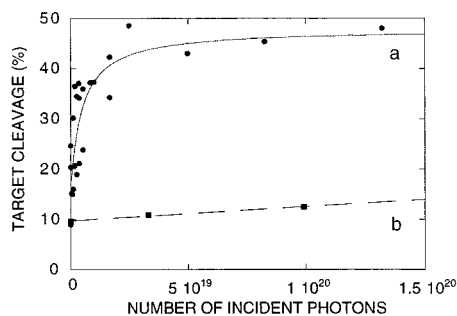


**Figure 9.** Dependence on light intensity of the site-directed cleavage (positions 13–26) of the 41-mer hairpin after piperidine treatment using the complementary TTCTTCTCCTTCT-CHEVP conjugate (a) and the noncomplementary CGGCAGCCACAC-CHEVP conjugate (b). The results from three independent experiments have been cumulated in (a).

noting that the most reactive guanines were those located in the single-stranded loop region of the hairpin target. A higher sensitivity to photocleavage by hematoporphyrin of single-stranded DNA, as compared to double-stranded DNA, was previously pointed out.<sup>25</sup>

In order to further substantiate that the photodamages were site-directed through coupling of the chlorin to the oligonucleotide, a control experiment was designed. The most obvious control, the effect of the free chlorin, was not feasible because this molecule was not soluble in water. Instead, we used a chlorin conjugate with the oligonucleotide CGGCAGCCACAC which cannot form a triple helix with our target. The results, which are shown in Figure 9, clearly confirm the above view. Other control experiments using the complementary oligonucleotide not coupled to the chlorin (not shown) also failed to induce any photocleavage.

The results obtained with the single-stranded target were qualitatively similar to those described above.

The site-directed DNA cleavage patterns obtained with the chlorin conjugate were very similar to those obtained with oligonucleotide-fullerene conjugates.<sup>11</sup> The cleavage sites were located in the region of the target expected from the known orientation of the oligonucleotide conjugate: an antiparallel orientation with respect to the complementary strand in the duplex, an orientation parallel to the oligopurine target sequence in the triplex structures. The mobility of the bands in the gel also indicated that the cleavage occurred with generation of 3'-phosphorylated products.

**Photocleavage Quantum Yield.** As shown in Figure 9, the targeted cleavage leveled off around 50% for the highest light fluence. In keeping with previous observations,<sup>9</sup> this behavior might be due to photodegradation of the conjugate. Alteration of nucleic bases reducing the affinity of the conjugate for its target as well as photobleaching of the chlorin are likely to arise.

Therefore, the most significant value of the photocleavage quantum yield was that obtained for initial irradiation. Experiments were carried out using a 10.4% neutral filter in order to reduce the light intensity. The results are shown in Figure 8. In order to facilitate extrapolation, the data were tentatively fitted by the relation

$$y = ax/(bx + 1) + c \quad (6)$$

The parameter  $c$  accounts for some initial degradation of the target which may arise from unavoidable exposure of the sample to room light during handling, although maximum care was taken. The parameter  $a$  corresponds to the initial linear dependence of cleavage on the irradiation time, i.e., the value of interest, and  $a/b$  corresponds to the plateau value. Equation 6 has no theoretical basis and was used as a model to derive more reliable value of the parameter  $a$ .

Equation 5 which was derived in the material and method section can be rewritten as

$$P_r = 2.3 \times 10^5 \Phi \epsilon I_{ost} t / N \quad (7)$$

where  $I_{ost}$  is the fluence rate expressed as a number of photons per  $cm^2$  and per second and  $t$  is the irradiation time. In the experiment shown in Figure 8, the fluence rate  $I_{ost}$  was  $2.82 \times 10^{15}$  and  $5.73 \times 10^{15}$  photons  $s^{-1} cm^{-2}$  at 428 and 668 nm, respectively. In order to derive the quantum yield, the  $\epsilon$  value at the irradiation wavelength must be known. As the absorption spectrum of the chlorin was little affected by coupling with the oligonucleotide (Figure 3), it was assumed that typical values of 35 000 and 70 000  $M^{-1} cm^{-1}$  can be retained for the red and Soret bands, respectively.<sup>15</sup> Then, the quantum yield can be derived from the value of the parameter  $a$ . The quantum yields thus obtained for irradiation at 428 and 668 nm were very close,  $0.95 \times 10^{-3}$  and  $1.02 \times 10^{-3}$ , respectively.

**Investigation of the Photocleavage Mechanism.** The effect of oxygen on the photocleavage of the 41-mer hairpin structure was first examined. Two parallel experiments were conducted either on aerated or deoxygenated samples. The damages on the target were analyzed by electrophoresis on denaturing gels before or after piperidine treatment as described above and the cleavage quantified for each site. When oxygen was excluded, the cleavage did not exceed the background level, and no sequence specificity was seen. The results are shown in Figure 10a,b for piperidine treated samples. Clearly, oxygen is involved in the site-directed photocleavage of the target.

The reaction mechanism was further investigated using usual tests for singlet oxygen. As depicted in Figure 10c, sodium azide was found to inhibit the photocleavage reaction. The extent of inhibition attained about 50% at the most reactive site, i.e., the guanine 20. On the other hand, no increase of the yield of photocleavage was found in  $D_2O$ .

**Discussion.** It is worth noting that the photocleavage quantum yield was independent on the excitation wavelength. This excluded possible electron transfer from upper excited singlet states of the chlorin. The chlorin triplet state is most likely involved. In this excited state, the chlorin may either sensitize singlet oxygen formation or react with bases by electron transfer. Singlet oxygen was found to induce piperidine-labile

(25) Kawanishi, S.; Inoue, S.; Sano, S.; Aiba, H. *J. Biol. Chem.* **1986**, *261*, 6090–6095.

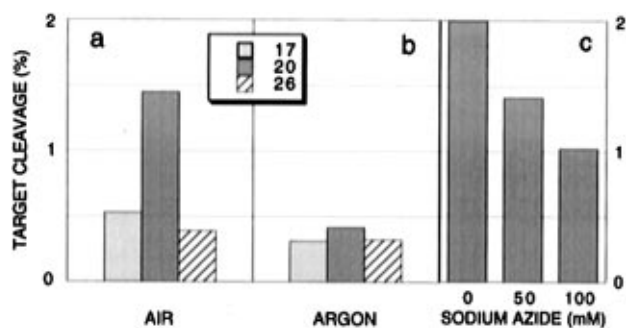


**Figure 10.** Photocleavage of double-stranded oligonucleotide with hairpin structure (Figure 6, structure 3) by the TTCTTCTCCTTTCT-CHEVP conjugate which forms a triple helix with its target. The cleavage at each guanine site (indicated in the figure) was computed as the ratio of the radioactivity counted in the corresponding band versus the total radioactivity. Samples were treated with piperidine. The samples were irradiated using 668 nm light (11 mW/cm<sup>2</sup>) for 6 min in experiments a, b and 8 min for experiment c. Other conditions were as in Figure 7: (a,b) effect of oxygen and (c) effect of NaN<sub>3</sub> as a quencher.

sites as well as strand breaks in DNA in a ratio of about 4/1.<sup>26</sup> In keeping with a higher reactivity of singlet oxygen with guanine as compared to the other bases,<sup>25,27</sup> cleavage was preferentially found at guanine residues. Also, single-stranded DNA was much more sensitive than double-stranded DNA. The present results obtained with the oligonucleotide-chlorin conjugate could be thus explained by reaction of singlet oxygen. In support to this conclusion, the role of oxygen and quenching by sodium azide are clearly demonstrated in Figure 10. It might be argued that during its lifetime in water (about 4  $\mu$ s) singlet oxygen may diffuse far from the chlorin moiety leading to damages that are not sequence-specific. This argument is likely invalid. Indeed, it must be emphasized that the quantum yield of photocleavage we have determined ( $\approx 10^{-3}$ ) is fairly low. Such a value can be expected for the reaction of singlet oxygen in the solvent cage formed around the photosensitizer and neighboring nucleic bases. A related situation is found in the autooxidation of rubrene, a photosensitizer which reacts back with singlet oxygen leading to an endoperoxide. At low rubrene concentration, the endoperoxide is produced by a re-encounter process involving the same rubrene molecule that has participated in the production of the singlet oxygen molecule.<sup>28</sup> In this system, the quantum yield of photooxidation was also found to be around  $10^{-3}$ . Assuming that singlet oxygen is reacting in the solvent cage formed around the photosensitizer, it is not surprising that the D<sub>2</sub>O effect, which is based on an increase of the singlet oxygen lifetime in the bulk solution, was not observed.

(26) Blazek, E. R.; Peak, J. G.; Peak, M. J. *Photochem. Photobiol.* **1989**, *49*, 607–613.

(27) Rougée, R.; Bensasson, R. V. *C. R. Acad. Sci. Paris* **1986**, *302*, 1223–1226.

(28) Aubry, J. M.; Rigaudy, J.; Cuong N. K. *Photochem. Photobiol.* **1981**, *33*, 155–158.

(29) Le Doan, T.; Perrouault, L.; Asseline, U.; Thuong, N. T.; Rivalle, C.; Bisagni, E.; Hélène, C. *Antisense Res. Dev.* **1991**, *1*, 43–54.

However, the experiments performed in deoxygenated solutions or with sodium azide are not sufficient to exclude mechanisms involving electron transfer and radical reactions. Indeed, oxygen might be involved in the formation of peroxy radicals following electron transfer. Likewise, sodium azide might also quench the triplet state of the photosensitizer.

Conjugates of oligonucleotides with various light-activable molecules have been described.<sup>9,11,29</sup> However, most of them must be excited by wavelengths strongly absorbed by blood and tissues. Compared to molecules such as aromatic azides, porphyrins, ellipticines, and fullerene, chlorins present the advantage of a strong absorption in the far-red making them better candidates for therapeutic applications. In this regard, it is interesting to compare the efficiency of oligonucleotides conjugated with chlorin and with fullerene.<sup>11</sup> The targets used for the two conjugates were essentially the same. Both molecules are efficient singlet oxygen photosensitizers.<sup>30,31</sup> Although the cleavage patterns obtained with both conjugates were similar, much longer irradiation times were required with the fullerene conjugate to produce the same effect. The difference is likely to reside in the important difference in absorption in the visible region between the two molecules.

A chlorin molecule related to those used in the present work has been shown to efficiently photoinactivate free human immunodeficiency viruses in blood.<sup>32</sup> Coupling such photosensitizers with oligonucleotides might make it possible to approach the problem of infected cells according to well-known strategies designed to inhibit gene expression at the translational or at the transcriptional levels.<sup>1–3</sup> In addition, owing to their hydrophobic character, chlorins, such as CHEVP, might improve interactions with membranes and increase cellular uptake as already observed with nonionic porphyrins or cholesterol.<sup>33</sup>

In conclusion, chlorin-oligonucleotide conjugates are promising compounds able to selectively induce damages to specific nucleic sequences. To our knowledge, the photochemical quantum yield of the damages, a critical value to elucidate mechanisms, has been determined for the first time for this class of compounds. The modest value of this quantum yield is largely compensated by the strong absorption of the chlorin moiety in the far red making these conjugates potential candidates for phototherapeutic applications.

**Acknowledgment.** This work was supported by the Agence Nationale de Recherche sur le SIDA (ANRS).

JA9600621

(30) Brault, D.; Vever-Bizet, C.; Rougée, M.; Bensasson, R. *Photochem. Photobiol.* **1988**, *47*, 151–154.

(31) Arbogast, J. W.; Darmany, A. P.; Foote, C. S.; Rubin, Y.; Diederich, F. N.; Alvarez, M. M.; Anz S. J.; Whetten R. L. *J. Am. Chem. Soc.* **1991**, *95*, 11–12.

(32) Grandadam, M.; Ingrand, D.; Huraux, J.-M.; Aveline, B.; Delgado, O.; Vever-Bizet, C.; Brault, D. *J. Photochem. Photobiol. B: Biol.*, **1995**, *31*, 171–177.

(33) Boutorine, A. S.; Boiziau, C.; Le Doan, T.; Toulmé, J. J.; Hélène, C. *Biochimie* **1992**, *74*, 485–489.